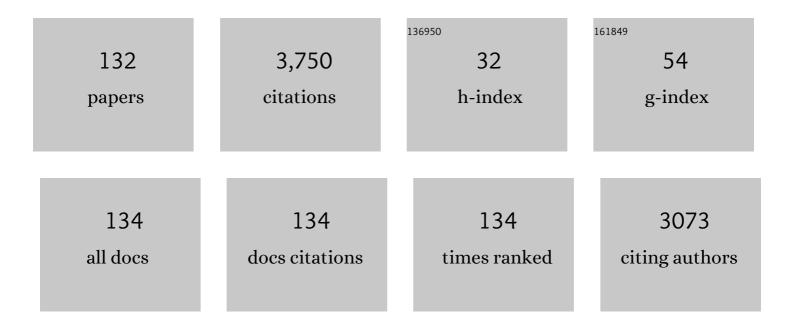
List of Publications by Year in descending order

Source: https://exaly.com/author-pdf/9327223/publications.pdf Version: 2024-02-01



IONC-HOLEE

#	Article	IF	CITATIONS
1	A 5 × 5 cm2 protonic ceramic fuel cell with a power density of 1.3 W cm–2 at 600 °C 3, 870-875.	. Nature E 39.5	nergy, 2018
2	Demonstrating the potential of yttrium-doped barium zirconate electrolyte for high-performance fuel cells. Nature Communications, 2017, 8, 14553.	12.8	218
3	Highâ€Performance Microâ€Solid Oxide Fuel Cells Fabricated on Nanoporous Anodic Aluminum Oxide Templates. Advanced Functional Materials, 2011, 21, 1154-1159.	14.9	151
4	Extremely Thin Bilayer Electrolyte for Solid Oxide Fuel Cells (SOFCs) Fabricated by Chemical Solution Deposition (CSD). Advanced Materials, 2012, 24, 3373-3377.	21.0	118
5	The potential and challenges of thin-film electrolyte and nanostructured electrode for yttria-stabilized zirconia-base anode-supported solid oxide fuel cells. Journal of Power Sources, 2014, 247, 105-111.	7.8	104
6	Nano-tailoring of infiltrated catalysts for high-temperature solid oxide regenerative fuel cells. Nano Energy, 2017, 36, 9-20.	16.0	88
7	Role of Multivalent Pr in the Formation and Migration of Oxygen Vacancy in Pr-Doped Ceria: Experimental and First-Principles Investigations. Chemistry of Materials, 2012, 24, 4261-4267.	6.7	86
8	Low Temperature Performance Improvement of SOFC with Thin Film Electrolyte and Electrodes Fabricated by Pulsed Laser Deposition. Journal of the Electrochemical Society, 2009, 156, B1484.	2.9	78
9	Superionic Halogen-Rich Li-Argyrodites Using In Situ Nanocrystal Nucleation and Rapid Crystal Growth. Nano Letters, 2020, 20, 2303-2309.	9.1	75
10	Fabrication and performance evaluation of 3-cell SOFC stack based on planar 10cm×10cm anode-supported cells. Journal of Power Sources, 2006, 159, 478-483.	7.8	71
11	Low temperature sintering of BaZrO3-based proton conductors for intermediate temperature solid oxide fuel cells. Solid State Ionics, 2010, 181, 163-167.	2.7	69
12	Microstructural factors of electrodes affecting the performance of anode-supported thin film yttria-stabilized zirconia electrolyte (â^¼1̼m) solid oxide fuel cells. Journal of Power Sources, 2011, 196, 7169-7174.	7.8	65
13	Suppression of Ni agglomeration in PLD fabricated Ni-YSZ composite for surface modification of SOFC anode. Journal of the European Ceramic Society, 2010, 30, 3415-3423.	5.7	61
14	Synthesis of nano-crystalline Ce0.9Gd0.1O1.95 electrolyte by novel sol–gel thermolysis process for IT-SOFCs. Journal of the European Ceramic Society, 2008, 28, 3107-3112.	5.7	60
15	Impact of nanostructured anode on low-temperature performance of thin-film-based anode-supported solid oxide fuel cells. Journal of Power Sources, 2016, 315, 324-330.	7.8	60
16	Effect of nickel nano-particle sintering on methane reforming activity of Ni-CGO cermet anodes for internal steam reforming SOFCs. Applied Catalysis B: Environmental, 2011, 101, 531-539.	20.2	57
17	The effect of an ultra-thin zirconia blocking layer on the performance of a 1-μm-thick gadolinia-doped ceria electrolyte solid-oxide fuel cell. Journal of Power Sources, 2012, 206, 91-96.	7.8	57
18	Catalytic behavior of metal catalysts in high-temperature RWGS reaction: In-situ FT-IR experiments and first-principles calculations. Scientific Reports, 2017, 7, 41207.	3.3	57

#	Article	IF	CITATIONS
19	Investigation of anode-supported SOFC with cobalt-containing cathode and GDC interlayer. Solid State Ionics, 2008, 179, 1535-1539.	2.7	56
20	Highly Dense Mn-Co Spinel Coating for Protection of Metallic Interconnect of Solid Oxide Fuel Cells. Journal of the Electrochemical Society, 2014, 161, F1389-F1394.	2.9	55
21	Quantitative Analysis of Microstructures and Reaction Interfaces on Composite Cathodes in All-Solid-State Batteries Using a Three-Dimensional Reconstruction Technique. ACS Applied Materials & Interfaces, 2018, 10, 23740-23747.	8.0	53
22	Promotion of Pt/CeO ₂ catalyst by hydrogen treatment for low-temperature CO oxidation. RSC Advances, 2019, 9, 27002-27012.	3.6	53
23	High-performance thin-film protonic ceramic fuel cells fabricated on anode supports with a non-proton-conducting ceramic matrix. Journal of Materials Chemistry A, 2016, 4, 6395-6403.	10.3	52
24	Electrochemical analysis of high-performance protonic ceramic fuel cells based on a columnar-structured thin electrolyte. Applied Energy, 2019, 233-234, 29-36.	10.1	52
25	Physical and Microstructural Properties of NiO―and Ni‥SZ Composite Thin Films Fabricated by Pulsed‣aser Deposition at <i>T</i> ≤00°C. Journal of the American Ceramic Society, 2009, 92, 3059-3064.	3.8	45
26	Three dimensional representations of partial ionic and electronic conductivity based on defect structure analysis of BaZr0.85Y0.15O3â''. Solid State Ionics, 2011, 203, 9-17.	2.7	44
27	Praseodymium doped ceria as electrolyte material for IT-SOFC applications. Materials Chemistry and Physics, 2018, 216, 136-142.	4.0	42
28	â€ĩllusional' nano-size effect due to artifacts of in-plane conductivity measurements of ultra-thin films. Physical Chemistry Chemical Physics, 2011, 13, 6133.	2.8	41
29	Thermo-mechanical stability of multi-scale-architectured thin-film-based solid oxide fuel cells assessed by thermal cycling tests. Journal of Power Sources, 2014, 249, 125-130.	7.8	39
30	Synthesis, sintering and conductivity behavior of ceria-doped Scandia-stabilized zirconia. Solid State Ionics, 2014, 263, 103-109.	2.7	37
31	Highly active and thermally stable single-atom catalysts for high-temperature electrochemical devices. Energy and Environmental Science, 2020, 13, 4903-4920.	30.8	35
32	Optimization of current collection to reduce the lateral conduction loss of thin-film-processed cathodes. Journal of Power Sources, 2013, 230, 109-114.	7.8	34
33	Effect of sintering atmosphere on phase stability, and electrical conductivity of proton-conducting Ba(Zr0.84Y0.15Cu0.01)O3â^'. International Journal of Hydrogen Energy, 2014, 39, 7100-7108.	7.1	34
34	Protonic ceramic electrolysis cells for fuel production: a brief review. Journal of the Korean Ceramic Society, 2020, 57, 480-494.	2.3	34
35	Pulsed Laser Deposition of La0.6Sr0.4CoO3â~'δ-Ce0.9Gd0.1O2â~'δ Nano-Composite and Its Application to Gradient-Structured Thin-film Cathode of SOFC. Journal of the Electrochemical Society, 2011, 158, B1000.	2.9	32
36	Enhanced oxygen diffusion in epitaxial lanthanum–strontium–cobaltite thin film cathodes for micro solid oxidefuel cells. Energy and Environmental Science, 2013, 6, 116-120.	30.8	32

#	Article	IF	CITATIONS
37	Thin film yttria-stabilized zirconia electrolyte for intermediate-temperature solid oxide fuel cells (IT-SOFCs) by chemical solution deposition. Journal of the European Ceramic Society, 2012, 32, 1733-1741.	5.7	30
38	SOFCs with Sc-Doped Zirconia Electrolyte and Co-Containing Perovskite Cathodes. Journal of the Electrochemical Society, 2007, 154, B480.	2.9	29
39	An investigation of the interfacial stability between the anode and electrolyte layer of LSGM-based SOFCs. Journal of Materials Science, 2007, 42, 1866-1871.	3.7	29
40	Sintering behavior and electrochemical performances of nano-sized gadolinium-doped ceria via ammonium carbonate assisted co-precipitation for solid oxide fuel cells. Journal of Alloys and Compounds, 2016, 682, 188-195.	5.5	29
41	Fabrication of anode-supported protonic ceramic fuel cell with Ba(Zr0.85Y0.15)O3â^–Ba(Ce0.9Y0.1)O3â^' dual-layer electrolyte. International Journal of Hydrogen Energy, 2014, 39, 12812-12818.	7.1	28
42	Highly durable solid oxide fuel cells: suppressing chemical degradation <i>via</i> rational design of a diffusion-blocking layer. Journal of Materials Chemistry A, 2018, 6, 15083-15094.	10.3	28
43	Grain size effect on the electrical properties of nanocrystalline ceria. Journal of the European Ceramic Society, 2014, 34, 2363-2370.	5.7	27
44	Scale-Up of Thin-Film Deposition-Based Solid Oxide Fuel Cell by Sputtering, a Commercially Viable Thin-Film Technology. Journal of the Electrochemical Society, 2016, 163, F613-F617.	2.9	27
45	Effect of secondary metal catalysts on butane internal steam reforming operation of thin-film solid oxide fuel cells at 500–600 °C. Applied Catalysis B: Environmental, 2020, 263, 118349.	20.2	27
46	Limitation of Thickness Increment of Lanthanum Strontium Cobaltite Cathode Fabricated by Pulsed Laser Deposition. Journal of the Electrochemical Society, 2011, 158, B1.	2.9	24
47	Lattice distortion effect on electrical properties of GDC thin films: Experimental evidence and computational simulation. Solid State Ionics, 2012, 229, 45-53.	2.7	24
48	Lattice-strain effect on oxygen vacancy formation in gadolinium-doped ceria. Journal of Electroceramics, 2014, 32, 72-77.	2.0	24
49	Fabrication of thin-film gadolinia-doped ceria (GDC) interdiffusion barrier layers for intermediate-temperature solid oxide fuel cells (IT-SOFCs) by chemical solution deposition (CSD). Ceramics International, 2014, 40, 8135-8142.	4.8	24
50	Synthesis of GDC electrolyte material for IT-SOFCs using glucose & fructose and its characterization. Nano Structures Nano Objects, 2017, 11, 7-12.	3.5	24
51	Study on the Electrode Reaction Mechanism of Pulsed-Laser Deposited Thin-Film La _{1â^'x} Sr _x CoO _{3â^'Î} (x = 0.2. 0.4) Cathodes. Journal of the Electrochemical Society, 2012, 159, F639-F643.	2.9	23
52	Chemically Evolved Composite Lithium-Ion Conductors with Lithium Thiophosphates and Nickel Sulfides. ACS Energy Letters, 2017, 2, 1740-1745.	17.4	23
53	Reassessment of conventional polarization technique to measure partial electronic conductivity of electrolytes. Solid State Ionics, 2010, 181, 724-729.	2.7	22
54	Soot Oxidation Activity of Redox and Non-Redox Metal Oxides Synthesised by EDTA–Citrate Method. Catalysis Letters, 2017, 147, 3004-3016.	2.6	22

#	Article	IF	CITATIONS
55	Substrate effect on the electrical properties of sputtered YSZ thin films for co-planar SOFC applications. Journal of Electroceramics, 2010, 24, 153-160.	2.0	21
56	Effect of Elastic Network of Ceramic Fillers on Thermal Cycle Stability of a Solid Oxide Fuel Cell Stack. Advanced Energy Materials, 2012, 2, 461-468.	19.5	21
57	Optical absorption and XPS studies of (Ba 1â^'x Sr x)(Ce 0.75 Zr 0.10 Y 0.15)O 3â^'î´ electrolytes for protonic ceramic fuel cells. Ceramics International, 2016, 42, 10366-10372.	4.8	21
58	Transmission Electron Microscopy Study on Microstructure and Interfacial Property of Thin Film Electrolyte SOFC. Electrochemical and Solid-State Letters, 2011, 14, B26.	2.2	20
59	Influence of background oxygen pressure on film properties of pulsed laser deposited Y:BaZrO3. Thin Solid Films, 2014, 552, 24-31.	1.8	20
60	Palladium incorporation at the anode of thin-film solid oxide fuel cells and its effect on direct utilization of butane fuel at 600â€Â°C. Applied Energy, 2019, 243, 155-164.	10.1	20
61	Atomistic Assessments of Lithium-Ion Conduction Behavior in Glass–Ceramic Lithium Thiophosphates. ACS Applied Materials & Interfaces, 2019, 11, 13-18.	8.0	20
62	Fabrication of dense and defect-free diffusion barrier layer via constrained sintering for solid oxide fuel cells. Journal of the European Ceramic Society, 2017, 37, 3219-3223.	5.7	19
63	Incorporation of a Pd catalyst at the fuel electrode of a thin-film-based solid oxide cell by multi-layer deposition and its impact on low-temperature co-electrolysis. Journal of Materials Chemistry A, 2017, 5, 7433-7444.	10.3	19
64	Sintered powder-base cathode over vacuum-deposited thin-film electrolyte of low-temperature solid oxide fuel cell: Performance and stability. Electrochimica Acta, 2019, 296, 1055-1063.	5.2	19
65	Solid oxide fuel cells with zirconia/ceria bilayer electrolytes via roll calendering process. Journal of Alloys and Compounds, 2020, 846, 156318.	5.5	19
66	Integrated application of semantic segmentation-assisted deep learning to quantitative multi-phased microstructural analysis in composite materials: Case study of cathode composite materials of solid oxide fuel cells. Journal of Power Sources, 2020, 471, 228458.	7.8	19
67	Estimation of the protonic concentration and mobility in Ba(Zr0.81Yb0.15Zn0.04)O3â~δ ceramic. Solid State Ionics, 2011, 192, 88-92.	2.7	18
68	Fabrication and characterization of Ba(Zr0.84Y0.15Cu0.01)O3 electrolyte-based protonic ceramic fuel cells. Ceramics International, 2013, 39, 9605-9611.	4.8	18
69	Oxygen ion transport in doped ceria: effect of vacancy trapping. Journal of Materials Chemistry A, 2021, 9, 13883-13889.	10.3	18
70	Thermally Induced S-Sublattice Transition of Li ₃ PS ₄ for Fast Lithium-Ion Conduction. Journal of Physical Chemistry Letters, 2018, 9, 5592-5597.	4.6	17
71	Improved electrochemical performance and durability of butaneâ€operating lowâ€temperature solid oxide fuel cell through palladium infiltration. International Journal of Energy Research, 2020, 44, 9995-10007.	4.5	17
-	Physical and Electrochemical Characteristics of Pulsed Laser Deposited	Î develec New	

72 La_{0.6}Sr_{0.4}CoO_{3â^{*}Î}-Ce_{0.9}Gd_{0.1}O_{2â^{*}Î} Nanocomposites as a Function of the Mixing Ratio. Journal of the Electrochemical Society, 2014, 161, F16-F22.

#	Article	IF	CITATIONS
73	Naturally diffused sintering aid for highly conductive bilayer electrolytes in solid oxide cells. Science Advances, 2021, 7, eabj8590.	10.3	16
74	Effect of Ba-deficiency on the phase and structural stability of (BaSr)(CeZr)O3-based proton conducting oxides. International Journal of Hydrogen Energy, 2015, 40, 11022-11031.	7.1	15
75	A nanoarchitectured cermet composite with extremely low Ni content for stable high-performance solid oxide fuel cells. Acta Materialia, 2021, 206, 116580.	7.9	15
76	Influence of sintering activators on electrical property of BaZr0.85Y0.15O3-Î′ proton-conducting electrolyte. Journal of Power Sources, 2021, 507, 230296.	7.8	15
77	Tailoring shape and exposed crystal facet of single-crystal layered-oxide cathode particles for all-solid-state batteries. Chemical Engineering Journal, 2022, 445, 136828.	12.7	15
78	The Effect of Post-Annealing on the Properties of a Pulsed-Laser-Deposited La _{0.6} Sr _{0.4} CoO _{3-δ} Ce _{0.9} Gd _{0.1} O _{2-δCathode. Journal of the Electrochemical Society, 2013, 160, F1027-F1032.}	o>⊠aano-Co	omposite
79	Processing and characterizations of a novel proton-conducting BaCe0.35Zr0.50Y0.15O3-δ electrolyte and its nickel-based anode composite for anode-supported IT-SOFC. Materials for Renewable and Sustainable Energy, 2014, 3, 1.	3.6	14
80	Interpretation of Impedance Spectra of Solid Oxide Fuel Cells: L-Curve Criterion for Determination of Regularization Parameter in Distribution Function of Relaxation Times Technique. Jom, 2019, 71, 3825-3834.	1.9	14
81	Constrained Sintering in Fabrication of Solid Oxide Fuel Cells. Materials, 2016, 9, 675.	2.9	13
82	Deep learning-assisted microstructural analysis of Ni/YSZ anode composites for solid oxide fuel cells. Materials Characterization, 2021, 172, 110906.	4.4	12
83	Achieving performance and longevity with butane-operated low-temperature solid oxide fuel cells using low-cost Cu and CeO ₂ catalysts. Journal of Materials Chemistry A, 2022, 10, 2460-2473.	10.3	12
84	Structural optimization of (La, Sr)CoO3-based multilayered composite cathode forÂsolid-oxide fuel cells. Journal of Power Sources, 2013, 228, 97-103.	7.8	11
85	Sandwiched ultra-thin yttria-stabilized zirconia layer to effectively and reliably block reduction of thin-film gadolinia-doped ceria electrolyte. Journal of the Ceramic Society of Japan, 2015, 123, 263-267.	1.1	11
86	Identification of an Actual Strain-Induced Effect on Fast Ion Conduction in a Thin-Film Electrolyte. Nano Letters, 2018, 18, 2794-2801.	9.1	11
87	Comprehensive Understanding of Cathodic and Anodic Polarization Effects on Stability of Nanoscale Oxygen Electrode for Reversible Solid Oxide Cells. ACS Applied Materials & Interfaces, 2018, 10, 39608-39614.	8.0	11
88	Robust solid-state interface with a deformable glass interlayer in sulfide-based all-solid-state batteries. Solid State Ionics, 2020, 346, 115217.	2.7	11
89	Quantitative determination of lithium depletion during rapid cycling in sulfide-based all-solid-state batteries. Chemical Communications, 2021, 57, 3453-3456.	4.1	11
90	Ceria-samarium binary metal oxides: A comparative approach towards structural properties and soot oxidation activity. Molecular Catalysis, 2018, 451, 247-254.	2.0	10

#	Article	IF	CITATIONS
91	Roles of Polymerized Anionic Clusters Stimulating for Hydrolysis Deterioration in Li ₇ P ₃ S ₁₁ . Journal of Physical Chemistry C, 2021, 125, 19509-19516.	3.1	10
92	Strain-Induced Tailoring of Oxygen-Ion Transport in Highly Doped CeO ₂ Electrolyte: Effects of Biaxial Extrinsic and Local Lattice Strain. ACS Applied Materials & Interfaces, 2017, 9, 42415-42419.	8.0	10
93	The proton uptake process in double perovskite triple ionic-electronic conducting oxides for protonic ceramic cells. Journal of Materials Chemistry A, 2022, 10, 16127-16136.	10.3	10
94	Effects of B-site substitution on the surface adsorption properties and catalytic activities of La0.8Sr0.2(Mn1â^'xCox)O3. Applied Catalysis A: General, 2010, 387, 203-208.	4.3	9
95	Surface modification of anode substrate via nano-powder slurry spin coating for the thin film electrolyte of solid oxide fuel cell. Thin Solid Films, 2011, 519, 2534-2539.	1.8	9
96	Determination of proton transference number of Ba(Zr0.84Y0.15Cu0.01)O3â^î́r via electrochemical concentration cell test. Journal of Solid State Electrochemistry, 2013, 17, 2833-2838.	2.5	9
97	High-Temperature Current Collection Enabled by the in Situ Phase Transformation of Cobalt–Nickel Foam for Solid Oxide Fuel Cells. ACS Applied Materials & Interfaces, 2017, 9, 39407-39415.	8.0	9
98	Configuring PS <i>x</i> tetrahedral clusters in Li-excess Li7P3S11 solid electrolyte. APL Materials, 2018, 6, .	5.1	9
99	Effect of <scp>Fe</scp> infiltration to <scp>Ni</scp> / <scp>YSZ</scp> solidâ€oxideâ€cell fuel electrode on steam/ <scp>CO</scp> ₂ coâ€electrolysis. International Journal of Energy Research, 2019, 43, 4949-4958.	4.5	9
100	Enhanced sinterability and electrochemical performance of solid oxide fuel cells via a rollÂcalendering process. Journal of Materials Chemistry A, 2019, 7, 9958-9967.	10.3	9
101	PrBa0.5Sr0.5Co1.5Fe0.5O5+δ composite cathode in protonic ceramic fuel cells. Journal of the Korean Ceramic Society, 2021, 58, 351-358.	2.3	9
102	Thin Film (La _{0.7} Sr _{0.3}) _{0.95} MnO _{3-δ} Fabricated by Pulsed Laser Deposition and Its Application as a Solid Oxide Fuel Cell Cathode for Low-Temperature Operation. Journal of the Korean Ceramic Society, 2010, 47, 75-81.	2.3	9
103	Powder Packing Behavior and Constrained Sintering in Powder Processing of Solid Oxide Fuel Cells (SOFCs). Journal of the Korean Ceramic Society, 2019, 56, 130-145.	2.3	9
104	Effect of internal and external constraints on sintering behavior of thin film electrolytes for solid oxide fuel cells (SOFCs). Ceramics International, 2014, 40, 13131-13138.	4.8	8
105	Open-cell voltage and electrical conductivity of a protonic ceramic electrolyte under two chemical potential gradients. Physical Chemistry Chemical Physics, 2018, 20, 14997-15001.	2.8	8
106	Experimental evidence of tunable space-charge-layer-induced electrical properties of nanocrystalline ceria thin films. Physical Chemistry Chemical Physics, 2013, 15, 15632.	2.8	7
107	On the sol-gel synthesis and characterization of (BaSr)(CeZr)O3-based fuel cell electrolytes. Ionics, 2016, 22, 2529-2538.	2.4	6
108	Collateral hydrogenation over proton-conducting Ni/BaZr _{0.85} Y _{0.15} O _{3â^ʾĨ´} catalysts for promoting CO ₂ methanation. RSC Advances, 2018, 8, 32095-32101.	3.6	6

#	Article	IF	CITATIONS
109	High-performance and robust operation of anode-supported solid oxide fuel cells in mixed-gas atmosphere. International Journal of Energy Research, 2016, 40, 726-732.	4.5	5
110	Synthesis and conductivity behaviour of proton conducting (1â^' <i>x</i>)Ba _{0.6} Sr _{0.4} Ce _{0.75} Zr _{0.10} Y _{0.15(<i>x</i>=0, 0.2, 0.5) composite electrolytes. Journal of the American Ceramic Society, 2017, 100, 4710-4718.}	>O _{3â^}	Ί́â€≮sα
111	Suppression of processing defects in large-scale anode of planar solid oxide fuel cell via multi-layer roll calendering. Journal of Alloys and Compounds, 2020, 812, 152113.	5.5	5
112	Degradation of hydration kinetics of proton-conducting Ba(Zr0.84Y0.15Cu0.01)O3â^δ during conductivity-relaxation experiment. Journal of Power Sources, 2016, 332, 299-304.	7.8	4
113	Oxygen transport in epitaxial La0.875Sr0.125CoO3-Î′ thin-film cathodes for solid oxide fuel cells: Roles of anisotropic strain. Scripta Materialia, 2016, 115, 141-144.	5.2	4
114	Highly controlled thermal behavior of a conjugated gadolinia-doped ceria nanoparticles synthesized by particle-dispersed glycine-nitrate process. Journal of the European Ceramic Society, 2017, 37, 2159-2168.	5.7	4
115	Microstructural Characterization of Composite Electrode Materials in Solid Oxide Fuel Cells via Image Processing Analysis. Journal of the Korean Ceramic Society, 2010, 47, 86-91.	2.3	4
116	Fabrication of NiO-Y:BaZrO ₃ Composite Anode for Thin Film-Protonic Ceramic Fuel Cells using Tape-Casting. Journal of the Korean Ceramic Society, 2015, 52, 320-324.	2.3	4
117	Enhanced carbon tolerance of Ir alloyed Ni-Based metal for methane partial oxidation. Heliyon, 2018, 4, e00652.	3.2	3
118	Synthesis and investigation on stability and electrical conductivity of Ti-doped Ba3CaTa2-xTixO9 (0 â‰ ¤ €¯x â‰ ¤ €¯1.0) complex oxides. Journal of Alloys and Compounds, 2019, 775, 736-741.	5.5	3
119	Electrical Characterization of Ultrathin Film Electrolytes for Micro-SOFCs. Journal of the Korean Ceramic Society, 2012, 49, 404-411.	2.3	3
120	Microscopic Analysis of High Lithium-Ion Conducting Glass-Ceramic Sulfides. Journal of the Korean Ceramic Society, 2016, 53, 568-573.	2.3	3
121	Influence of wet atmosphere on electrical and transport properties of lanthanum strontium cobalt ferrite cathode materials for protonic ceramic fuel cells. Solid State Ionics, 2013, 249-250, 112-116.	2.7	2
122	Effects of mixing state of composite powders on sintering behavior of cathode for solid oxide fuel cells. Ceramics International, 2017, 43, 11642-11647.	4.8	2
123	Theoretical analysis of reversible phase evolution in Li-ion conductive halides. Applied Surface Science, 2022, 574, 151621.	6.1	2
124	Performance of Solid Oxide Fuel Cell with Gradient-structured Thin-film Cathode Composed of Pulsed-laser-deposited Lanthanum Strontium Manganite-Yttria-stabilized Zirconia Composite. Journal of the Korean Ceramic Society, 2011, 48, 487-492.	2.3	2
125	Experimental and computational analyses of ionic current leakage on the co-planar integrated fuel cells. Solid State Ionics, 2009, 180, 1534-1538.	2.7	1
126	Facile fabrication of YSZ/GDC multi-layers by using a split target in pulsed laser deposition and their structural and electrical properties. Journal of Electroceramics, 2014, 33, 25-30.	2.0	1

#	Article	IF	CITATIONS
127	Suppressing Lateral Conduction Loss of Thin-film Cathode by Inserting a Denser Bridging Layer. Journal of the Korean Ceramic Society, 2015, 52, 304-307.	2.3	1
128	Exploration of a Ce _{0.65} Zr _{0.25} Pr _{0.1} O _{2â~îî} -Based Electrocatalyst That Exhibits Rapid Performance Deterioration Despite Its High Oxygen Storage Capability. ACS Applied Energy Materials, 0, , .	5.1	1
129	Effects of Yb-Concentration on the Proton Conductivities of Low Temperature Sinterable Barium Zirconate Ceramics. Resources Processing, 2010, 57, 8-11.	0.4	0
130	Microstructure refinement of pulsed laser deposited La0.6Sr0.4CoO3â^î´ thin-film cathodes for solid oxide fuel cell. Metals and Materials International, 2013, 19, 1347-1349.	3.4	0
131	Effect of alumina nanofiller on the viscosity and electrical conductivity of glass-based seals for solid oxide fuel cells. Research on Chemical Intermediates, 2014, 40, 2423-2429.	2.7	0
132	Correlation between Fabrication and Operation Conditions for Ce _{1-X} Zr _x O _{2-σ} (x~0.2) Stability. ECS Meeting Abstracts, 2020, MA2020-02, 2593-2593.	0.0	0